Structural performance of a modified shear-head assembly for edge steel column embedded in reinforced concrete slab

Barisua Ebenezer Ngekpe[a*], Samuel Jonah Abbey[b], and Adegoke Omotayo Olubanwo[c]

[a]Rivers State University of Sciences and Technology, Nkpolu, Port Harcourt, Nigeria
[b]University of South Wales, UK
[c]School of Energy, Construction & Environment, Coventry University, Coventry, West Midlands, UK

A R T I C L E I N F O	A B S T R A C T
	This paper presents a study on the structural performance of a modified shear-head assembly for edge steel column embedded in reinforced concrete slab. The structural performance was investigated in terms of punching shear capacity of the reinforced concrete flat slab. The study consisted of a laboratory punching shear test on the contra-flexure bound slab of dimension 1060mm × 1250mm by 130mm thick in a reactant test frame using a 500kN load cell. Results of the experimental study was validated using finite element based numerical method. Both experimental and numerical results show that increase in tensile strength of concrete, increases punching shear capacity of the connection. It was also observed that punching shear failure of the connection depended largely on concrete shear strength. This study has also revealed that punching shear occurs when concrete shear strength is reached, irrespective of the robustness of the shear-head connection.

1. Introduction

Flat slab system is increasingly popular in the construction industry in recent time due to its structural and architectural merits. But punching shear failure at slab to column connection is a dominant source of structural damage and should therefore be considered in the design of flat slab. Punching shear failure, a local failure phenomenon, has been a subject of intense experimental, numerical and analytical investigations over the years. Reinforced Concrete structural elements can be made from different classifications of cement, with or without cementitious admixtures (Abbey et al., 2015, 2016, 2017; Piel, & Hanswille, 2006), Olubanwo et al. (2018). All design codes for punching shear emphasis reinforced concrete flat slab supported on RC column; which limits the applicability of steel column in flat slab design. However, the alternative use of steel column would require a special connection such as shear-head. Shear-head system is a pleasant alternative to punching shear enhancement for connecting flat slab to steel column. The application of shear-head systems was first proposed by Corley and Hawkins (1968) which was further implemented in the ACI design method (ACI 318-05). Again, ACI 318-05 design guidance is limited to RC column. Other researchers have

* Corresponding author.
E-mail addresses: aa7878@coventry.ac.uk (B. E. Ngekpe)

investigated the applicability of shear-head assembly in various loading scenarios against punching shear. Eder et.al (2010) conducted numerical and experimental investigations on punching shear of a hybrid flats slab with shear-heads. The study focused on the contribution of shear-head to punching shear capacity of the interior slab-column connection not transferring unbalanced moment. The shear-head was designed based on the ACI 318-05 recommendation. The shear-heads were welded to the tubular steel column and inserted between the layers of the reinforcement. It was observed that the shear-head deformed plastically before punching failure occurred. Eder et al. (2011) investigated the behaviour of ductile shear-heads for connecting reinforced concrete flat slabs to interior tubular steel columns. The structural response of the proposed shear-heads was compared to the conventional ACI-type shear-heads that is fully embedded in the slab. The proposed shear-head was designed as a dissipative element which yields in shear before punching failure occurs in the slab. In the conventional ACI shear-head system, a punching failure load of 450kN was recorded while in the proposed shear-head system, a punching failure load of 385kN was recorded. The early failure is attributed to the localized concrete failure at the intersection of the shear arms with edges of the opening near the column. In order to eliminate the localized concrete failure around the opening, it was recommended that the slab edge should be adequately reinforced around the opening. To achieve adequate ductility, the connection should have failed above the failure load obtained in the conventional ACI shear-head system. This result suggests that creating an opening near the column aggravates punching shear capacity of the connection which is undesirable. Based on the shortcomings of the previous test, Eder, et al. (2012) design a robust shear-head system for connecting reinforced concrete flat slabs to tubular steel columns. In order to eliminate the early localized concrete failure around the edges of the hole in the previous experiment, the hole was adequately reinforced with steel collar. The authors also performed tests on several steel sections such as: hollow rectangular section, PFC section, channel and I-section. Results of the tests revealed that I-section is the most suitable due to reduced depth of shear cone punched out of the concrete at failure. Besides, a good composite action was achieved using **I**-section. Both gravity and cyclic tests carried out failed on the connection, but punching shear did not occur due the ruggedness of the connection. Despite the great effort, punching shear capacity of the proposed shear-head assembly could not be ascertained because the connection did not fail in punching during the test and hence; the contribution of the shear arms was indeterminate. The authors suggested that the contribution of the shear arms could have been determined if the shear arms acted as a cantilever, like in the case of the fully embedded ACI shear-head system. It was concluded that **I**-section performs better as shear arms than any other sections due to improved composite action with the concrete slab. Xu et al. (2016) developed a nonlinear finite element model for the analysis of concrete-filled steel tubular circular hollow sections under axial tension. The modified mohr coulomb failure criterion was adopted as the failure criterion for steel. An equation was proposed that accounted for the shear stress distribution for punching shear. Yan and Wang (2016) performed a comprehensive parametric study to investigate the influence of different design parameters on the punching shear resistance of hybrid flat slab with shear-head to interior steel tubular column connection. Results obtained from their numerical simulation correlated well with the BS8110 and Eurocode 2 codes equations. Ngekpe et al. (2016) examines the applicability of Total strain crack model in punching shear modeling for slab to edge column connection without shear reinforcement. Parametric study revealed that concrete tensile strength and shear retention factor have significant influence on the punching shear failure load. Bompa and Elghazouli (2016) investigated the structural performance of hybrid members consisting of reinforced concrete flat slabs, with and without shear reinforcement, connected to steel columns by means of fully integrated shear-heads. Experimental results revealed that the behavior of the hybrid members is directly influenced by the shear-head properties as well as the amount of longitudinal reinforcement and transverse reinforcement. All specimens failed predominantly in punching shear. Test results were used for the development of analytical models which relates the rotational response, flexural strength and punching strength as a function of shear-head embedment length, layout and section size. Bompa and Elghazouli (2017) studied the performance of shear-head systems in hybrid RC flat slab to steel column systems via a series of numerical parametric assessments in which key influential materials and geometric parameters were investigated.

The result was used to assess the ultimate behavior in terms of both strength and deformation characteristics. Salient findings from both experimental and numerical analyses were used to improve the analytical models for hybrid slabs. Kim et al. (2014) developed a modified model for connection between RC flat slabs to CFT columns using shear-head. The model assumes the same force distribution obtained from RC flat–slab column behaviour. Genikomsou and Polak (2015) conducted nonlinear finite element analyses of reinforced concrete slab-column connections under static and pseudo-dynamic loadings to investigate punching shear failure. The damage plasticity model implemented in ABAQUS was adopted to define quasi-brittle concrete. Five interior slab-column specimens without shear reinforcement were analyzed. Two specimens of edge slab-column connections were also analyzed. The model was able to predict punching shear failure of tested slabs. Some researchers have studied cracking resistance of concrete parts and specimens (Nallathambi et al., 1986; Jenq & Shah 1985; Golewski et al., 2012; Fakhri et al., 2017). Wosatko et al. (2015) applied damage-plasticity models in finite element analysis of punching shear. An experimental investigation was carried out on interior column tested in punching for the purpose of validation of numerical models. Two inelastic constitutive models were adopted in the numerical simulations, namely: Gradient-enhanced damage plasticity model; and damaged plasticity model implemented in ABAQUS. Concrete plasticity model in ABAQUS incorporates the effect of moderate confining pressure and irreversible plastic damage. In ABAQUS, failure mechanism characteristics for quasi-brittle materials such as concrete is based on concrete plasticity in which yielding and plastic potential functions are used to represent material failure. Punching is preceded by tensile cracking. However, aggregate interlock, shear friction due to dowel action of reinforcement withstands substantial amount of the load after initial cracking. Also, the numerical predictions suggested a sharp brittle failure after initial cracking; which indicates that the post crack regime was not captured. Based on the available literature, there is a significant dearth of research on the applicability of shear-head connection to steel edge column. ACI 318-05 design guidance for shear-head connected to edge column is only applicable reinforced concrete column. Therefore, in this research paper, a modified shear-head assembly for edge steel column was implemented and proposed. Its structural response subjected to punching shear load was evaluated using numerical and experimental investigations. This Paper investigates the structural performance of shear-head assembly for connecting RC flat slab to steel edge column. Firstly, an experimental investigation was carried out to measure the punching shear capacity at the connection and the deformations of the shear-head. Secondly, a comprehensive numerical assessment was carried out using non-linear finite element procedures. The adopted modelling scheme is validated using previous research work of Eder et al. (2010). Following the success of the validation scheme, the model was further adopted to stimulate the behavior of the tested slab-column connection and also to undertake parametric assessments of some governing parameters of punching shear at the connection.

2. Methodology

2.1 Experimental Method

Normal concrete was made from Portland cement, sand and granite with a maximum aggregate size of $d_{max} = 20mm$. The materials used consisted of concrete, 5mm thick steel plate and I-section with section properties, $I_{x-x} = 5325684mm^4$, $S_{xx} = 16248mm^3$, $Z_{x-x} = 14014.95mm^3$. The 28days mean cylinder compressive strength value of concrete was $f'_c = 32.17 \, \text{N/mm}^2$ and the result of the elastic modulus test for control concrete specimens performed according to BS1881: part 121:19831 gave a value of 29.5 KN/mm². The punching shear capacity of the edge column was enhanced using shear-head and in strict compliance to the design recommendations of ACI318-14. The shear-head assembly was embedded in a reinforced concrete slab supported by edge steel column. Following the recommendations of ACI318-14, a shear-head was designed using a 5mm thick end plate, fillet-welded to the top and bottom flanges of the I- section. The end plate was designed to transfer forces uniformly from the flanges of the shear-head to the steel column. The shear-head was embedded in a reinforced concrete slab between the top and bottom reinforcement grids of 12 mm diameter bars and the bars intercepting with the shear arms and steel column were discontinued as shown in Fig. 1.
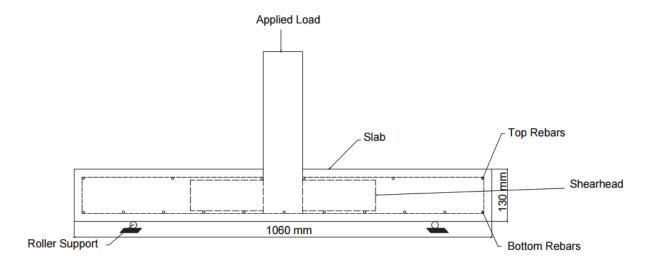
Fig. 1. shear-head inserted between reinforcement grid.

2.1.1 Test Set up and Instrumentation

Punching shear test was carried out on the contra-flexure bound slab of dimension 1060mm × 1250mm by 130mm thick in a reactant test frame. The test was set up using the same boundary conditions that captures the flexural behaviour of the slab, which was determined from the elastic analysis as depicted in Fig. 2. The elastic modulus and yield strength of reinforcement steel was assumed to be $210\,kN/mm^2$ and $500\,N/mm^2$ respectively, (BS EN, 10002). Strains were measured in the longitudinal direction of the shear arm using electrical resistance strain gauges (ESG). Axial strains were measured in the top and bottom flange with gauges positioned at 20 mm away from the intersection of the plate and shear arms. Shear strains were measured with strain gauge Rosettes positioned in the web of the shear arm. Concrete surface strains and strain across the concrete depth were measured using Demec strain gauge as shown in Fig. 2 and Fig. 3.
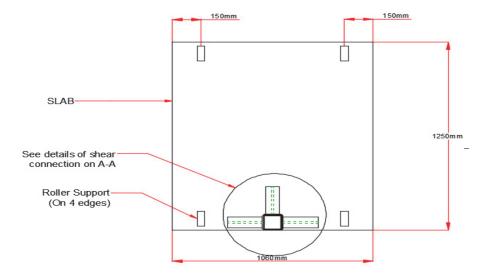

Fig. 2. Plan view of test set up.

Fig. 3. Shear-head assembly instrumented with strain gauges

A circular plate of diameter 150mm and thickness of 20mm was positioned between jack and steel column to ensure uniform distribution of load to the slab-column connection. The applied load was measured with a load cell 500 kN capacity, positioned between the hydraulic jack and steel plate. The load was applied incrementally at the rate of 10KN per minute and intervals strains across the slab depth were measured using DEMEC strain gauge. Vertical displacements were measured by means of three linear displacement transducers (LVDTs) placed directly underneath the plate that distributes the load uniformly from the hydraulic jack to the column.

2.2 Numerical Modelling

A numerical study of the slab-edge column-shear-head system was modelled using finite element based commercial software (Midas-FEA). The concrete slab was modelled using the 'Total strain crack model' based on the modified compression field theory of (Vecchio & Collin, 1986) and its 3D extension by (Selby & Vecchio, 1993) to account for the effect of lateral cracking. The concrete compressive behaviour is modelled with the parabolic softening model proposed by (Feenstra, 1993). The tensile behaviour of concrete was modelled with the exponential softening model in which the area of the softening zone equals G_f/h, where h is the crack bandwidth which is taken as $\sqrt[3]{V}$ (V = volume of element). The concrete tensile strength was taken as $f_c = 0.8 f_{cube}$ in accordance with EC 2 and the structural steel (shear-head) was modeled using four-node isoparametric shell element. Discrete embedded reinforcement concept was used to model the reinforcement and the steel was defined as perfectly elastic-plastic material based on Von mises yield criterion and perfect bond was assumed between reinforcement, embedded shear-heads and concrete. For computational efficiency, only half of the slab was modelled using the restraints to capture the flexural behavior of the isolated slab. Horizontal displacements were restrained in the X and Y directions on the axis of symmetry and along the edge of the slab parallel to the free edge; representing line of symmetry where maximum deflection occurred in prototype slab. Vertical displacement (Dz) was also allowed. The clamped was modelled by restraining the nodes near the supports. Rotational displacement was also applied on top of the column above the slab and at 150mm away from the right edge of the slab, a horizontal restrain in the Y-direction and vertical restrain were applied. Horizontal displacement in the X direction was allowed to replicate the behaviour of a roller support that was adopted in the experiment. The specimen was discretized into 16386 elements with 17693 nodes and the mesh was refined in the plan around the column and shear-heads. The material model properties and shear-heads section geometry are presented in Table 1.
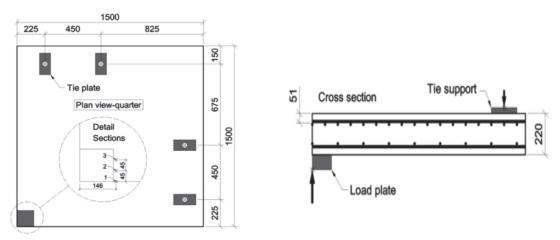
Table.1. Material model implemented in NLFEA.

Model	G_f (Nmm/mm^2)	G_c (Nmm/mm^2)	(β)	(Tensile softening)	(Compression softening)
Slab	0.074	7.4	0.3	exponential	parabolic

Section dimensions used for Shear arms in NLFEA

Section	h (mm)	w (mm)	t_f (mm)	t_w (mm)
I	76	3	3	3

Interface element was introduced to account for discrete cracking of concrete and loss of bond between the steel shear arm and concrete. The thickness of the interface was assumed zero and in order to overcome numerical instability associated with zero thickness interfaces, penalty stiffness ($K = 1000 \times E \times d$) was assigned. Where K = penalty stiffness, E =Elastic modulus of the stiffer element used in the model, in this case steel was used and d = representative element size. The interface element was assigned material properties, and then point interface type was adopted and a discrete crack interface was adopted to model the interfacial mechanism between the shear arm and the concrete because discrete cracking of concrete is expected around the shear-heard.

2.2.1 Numerical Model Validation

The finite element based commercial software (Midas-FEA) used in this study was validated using previous experimental study on a slab without shear reinforcement as tested by Vollum et al. (2009) cited in Eder et al. (2010). The slab is of 3m × 3m by 220mm thick, and loaded at the centre through a 270mm square plate with 16 ties located around its perimeter to restrain the slab in a vertical position. The bottom tensile reinforcement was spaced at 90mm centers and were used for tensile reinforcement at each orthogonal direction. The 10mm diameter bars were spaced at 180mm centers and used for compressive reinforcement at each orthogonal direction and a mean cylinder strength of 24Mpa was adopted. One-quarter plan view and reinforcement detail of the slab according to Vollum et.al (2009) are as shown in Fig. 4a and 4b respectively.

(a) Plan view (quarter section) (Eder et al., 2010)   (b) Reinforcement detail

Fig. 4(a-b). Slab plan view (quarter section) and reinforcement detail, (Eder et al., 2010; Vollum et al., 2009).

Due to symmetry and for computational efficiency, only a quarter of the specimen was modelled with the mesh refined around the column region where structural damages were expected to be more significant. In order to ensure that the quarter slab replicates the flexural behaviour of the full-scale

slab, horizontal displacements were restrained in the X and Y directions along the axis of symmetry. Vertical displacement was allowed for vertical deflection of the slab. The slab was vertically restrained at the positions of the tie down bars along its perimeter. The concrete and the element representing the steel column were modelled with 8-noded 3D solid element with the steel plate assumed as linear elastic material. The concrete was defined with the Total strain crack model and the reinforcement as elastic-plastic with the Von mises yield criterion. Embedded reinforcement concept was used and the slab was discretized into 19108 elements and 20942 nodes. A full integration scheme was adopted in the solution phase. The material properties and models used are as presented in Table 2 and Table 3.

Table 2. Material properties used in the model

Concrete (MPa)	$f_t = 1.5$	$E_c = 29500$
Steel (MPa)	$f_{yk} = 500$	$E_s = 210000$

Table 3. Material models adopted.

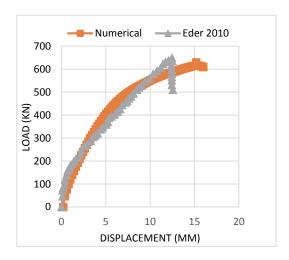|	Softening	$G_f(Nmm/mm^2)$	$G_c(Nmm/mm^2)$	β
Concrete in Tension	Exponential	0.074		0.3
Concrete in compression	Parabolic		7.4	0.3

G_f is the fracture energy in tension, G_c is fracture energy in compression and β is the shear retention factor.

3. Result and Discussion

3.1 Model validation results

In the first phase of the analysis the self-weight was activated to mimic the real life condition. In the second phase of the analysis, an incremental displacement load was applied from the bottom of the steel plate representing the column until punching shear failure occurred. Structural damages concentrate around the slab-column connection as shown in Fig. 5a. The Load displacement curve predicted using Midas FEA compares very well with the experimental result as shown in Fig. 5b.
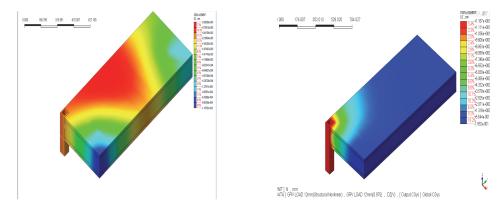

a) Deformation contour of the slab at failure load   b) Load-displacement curve

Fig. 5(a-b). Numerical model validation result and Eder et.al (2010) result

Fig. 4b shows that the experimental failure load occurred at 614 kN (Eder et al., 2010) while the numerical model validation failure load occurred at 629.08 kN, corresponding to about 2.4% fractional difference in failure load. In the present study, the comprehensive numerical simulation conducted on the tested slab agrees with experimental results. During the numerical modelling of the investigated slab of the current study, the self-weight was activated to check the deflection induced by self-weight. Fig. 6a, shows that under self-weight the deflection was maximum around the center of the slab as

expected. In the second phase of analysis, an incremental displacement load was applied from the base of the steel column, until punching shear failure of the slab occurred as shown in Fig. 6b. Local deformation was very significant at the slab-column connection as depicted in Fig. 6b, and it was observed that the shear-heads deformed plastically prior to punching shear failure.
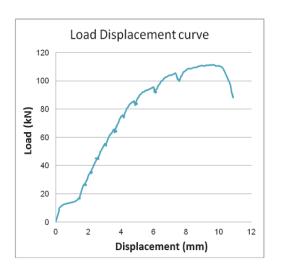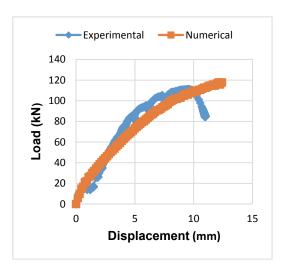

(a) Displacement contour of the tested slab under self-weight

(b) Displacement contour for the slab

Fig. 6. (a-b): Numerical model results of the investigated slab with shear-head

3.2 Load-displacement response

The Load displacement evolution measured by means of the LVDTs as shown in Fig. 7a shows that the load-displacement response becomes stiffer prior to the initiation of flexural cracks. The experimental failure load gives 111.35 kN while the numerical failure load gives 117.7 6kN as shown in Fig. 7b. In addition, it was observed that the summation of the self-weight and peak supports reaction equal the punching shear failure load. The numerical failure load deviated from the experimental failure load by 5.76%. A deviation of 12.98% was observed for displacement at failure load. These deviations may be attributed to the initiation of micro crack induced in the concrete due to restrained shrinkage during curing; which can reduce the elastic modulus and hence, reduction in stiffness of the concrete. An initial yielding of reinforcement occurred at a load of 90.62 kN, in the numerical model as shown in Fig. 8(a-b).
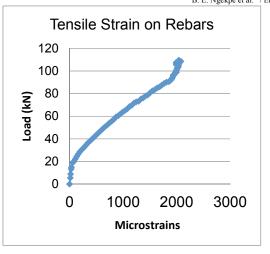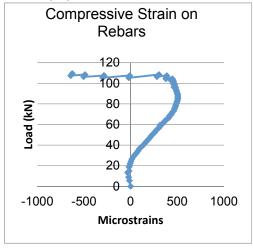

(a) Load displacement curve of LVDT

(b)Load-displacement curve for LVDT compared with numerical modelling result

Fig. 7(a-b). Load-displacement curve for LVDT and numerical modelling result

(a) Strain on tensile reinforcement   (b) Strain on compression rebars

Fig. 8(a-b). Reinforcement yielding

Reinforcement yielding occurred within the vicinity of the column and no other yielding zone was observed. This shows that structural deformations are concentrated within the vicinity of the column and this is consistent with experimental observation. An abrupt increase in strain value was observed for a load level corresponding roughly to the initiation of flexural cracks. The failure perimeter was difficult to measure in the test because crack propagated towards the column edges. The compressive face of the slab was almost intact; there was no significant crack propagation. From the observation, it could be tacitly assumed that punching shear failure occurs approximately when the shear strength of concrete is reached. This indicates that, regardless of the connection rigidity, punching shear failure may occur predominantly when the shear strength of concrete is reached. Earlier tests for shear-head connected to interior column performed by Corley et at (1968) revealed that shear-head increases punching capacity by enlarging the critical shear perimeter in similar way as the enlarged column.

3.2 Strains on Shear arms

Based on the yield strength and elastic modulus of steel assumed for the shear-head, an axial yield strain of -0.0017 was calculated; and compared with the axial compressive strain on the compression flange of shear arms for both measured and numerical models.
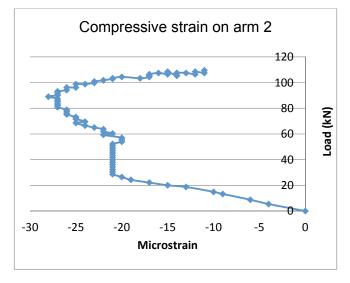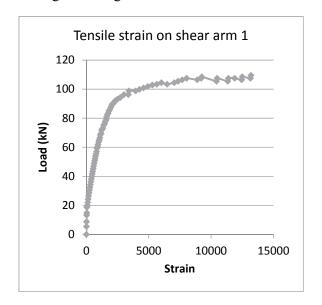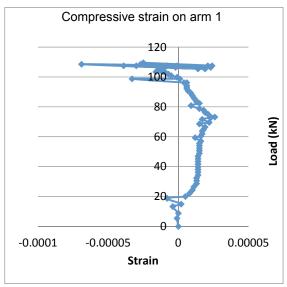

Fig. 9. Strain on compression flange of shear arm 2

The measured and numerical axial compressive strain was approximately -0.003, slightly above the calculated yield strain of -0.0017. This reveals that plastic deformation of the shear-head occurred prior to punching shear failure which is desirable. It could be observed that a similar evolution of compressive strain occurred under incremental loading for both experimental and numerical. The strain increases linearly between a load value of zero to 20kN and becomes approximately steady until punching shear failure occurred as shown in Fig. 9. The graph also shows that considerable bond was maintained between the shear-head and the concrete since there was no divergence. This is in line with the assumption of perfect bond between the embedded shear-head and concrete. The tensile and compressive strains on arm 1 is plotted in Fig. 10(a-b). The effect of shear arm length was also investigated using three different values of shear arm lengths (l_v) of 60, 120 and 185mm.

(a) Strain on tensile flange of shear arm 1   (b) Compressive strain (arm 1)

Fig. 10(a-b). Tensile and compressive strains on arm 1

The failure load increase as the shear arm length increases but there was no significant increase in displacement. The **I**-section shear arm was increased to an overall depth of 80mm. The thickness of its flanges and web were doubled to 6mm and that of the plate was increased to 10mm. This resulted to a significant increase in the failure load. This implies that increase in shear-heads, increases the punching shear capacity. The measured axial compressive strain (ε_x) -0.003 exceeded the theoretical yield strain of -0.015. This indicates that the shear-heads only deformed plastically before punching shear occurred which is desirable.

4. Conclusion

Results of both numerical and experimental investigations reveal that increase in tensile strength of concrete increases the punching shear capacity of the connection. Based on these results, it can be deduced that punching shear failure of the connection depends largely on concrete shear strength. Punching shear would likely occur when concrete shear strength is reached, despite the robustness of the shear-head connection. It can also be concluded that in a reinforced concrete slab with edge steel column, structural deformations are concentrated within the vicinity of the column.

Compliance with Ethical Standards

References

Abbey, S. J., Ngambi, S., & Coakley, E. (2016). Effect of Cement and by-product material inclusion on plasticity of deep mixing improved soils. *International Journal of Civil Engineering and Technology, 7*(5), 265-274.

Abbey, S. J., Ngambi, S., & Ngekpe, B. E. (2015). Understanding The Performance Of Deep Mixed Column Improved Soils-A Review. *International Journal of Civil Engineering and Technology (IJCIET)*, *6*(3), 97-117.

Abbey, S. J., Ngambi, S., & Olubanwo, A. O. (2017). Effect of overlap distance and chord angle on performance of overlapping soil-cement columns. *International Journal of Civil Engineering and Technology*, *8*(5), 627-637.

ACI318, Building Code Requirements for Structural Concrete (ACI 318M-14) and Commentary (ACI 318RM-14). Standard, American Concrete Institute (ACI), 2014.

ACI318. (2014) 'Building Code Requirements for Structural Concrete and Commentary', ACI, Detroit.

Bompa, D. V., & Elghazouli, A. Y. (2016). Structural performance of RC flat slabs connected to steel columns with shear heads. *Engineering Structures*, *117*, 161-183.

Bompa, D. V., & Elghazouli, A. Y. (2017). Numerical modelling and parametric assessment of hybrid flat slabs with steel shear heads. *Engineering Structures*, *142*, 67-83.

BS 8110 (1997).Structural use of concrete, part 1, code of practice for design and construction. London: British Standards Institution.

Chana, P. S., & Birjandi, F. K. (1996). Design guidance on structural steel shearheads in concrete. *Project report for Reinforced Concrete Council and Department of the Environment, CRIC CLIENT REPORT CRIC95/001/F, Imperial College London*.

Corley, W. G., & Hawkins, N. M. (1968, October). Shearhead reinforcement for slabs. In *Journal Proceedings* (Vol. 65, No. 10, pp. 811-824).

Eder, M. A., Vollum, R. L., Elghazouli, A. Y., & Abdel-Fattah, T. (2010). Modelling and experimental assessment of punching shear in flat slabs with shearheads. *Engineering Structures*, *32*(12), 3911-3924.

Eder, M. A., Vollum, R. L., & Elghazouli, A. Y. (2011). Inelastic behaviour of tubular column-to-flat slab connections. *Journal of Constructional Steel Research*, *67*(7), 1164-1173.

Eder, M. A., Vollum, R. L., & Elghazouli, A. Y. (2012). Performance of ductile RC flat slab to steel column connections under cyclic loading. *Engineering Structures*, *36*, 239-257.

Fakhri, M., Amoosoltani, E., & Aliha, M. R. M. (2017). Crack behavior analysis of roller compacted concrete mixtures containing reclaimed asphalt pavement and crumb rubber. *Engineering Fracture Mechanics*, *180*, 43-59.

Feenstra, P. H. (1993). Computational aspects of biaxial stress in plain and reinforced concrete. *PhD thesis, Delft University of Technology*.

Golewski, G. L., Golewski, P., & Sadowski, T. (2012). Numerical modelling crack propagation under Mode II fracture in plain concretes containing siliceous fly-ash additive using XFEM method. *Computational Materials Science*, *62*, 75-78.

Jenq, Y. S., & Shah, S. P. (1985). A fracture toughness criterion for concrete. *Engineering Fracture Mechanics*, *21*(5), 1055-1069.

Kim, J.W., Lee, C.H and Kang, T.H. (2014) 'Shearhead reinforcement for concrete slab to Concrete-filled tube column connections' ACI Struct J 111(3) 629–38.

Nallathambi, P., & Karihaloo, B. L. (1986). Determination of specimen-size independent fracture toughness of plain concrete. *Magazine of Concrete Research*, *38*(135), 67-76.

Ngekpe, B.E., Ode, T. & Eluozo, S.N. (2016). Application of total-strain crack model in finite element analysis for punching shear at edge connection. *International journal of Research in Engineering and Social Sciences 6*, (12), 1- 9.

Olubanwo, A. O., Karadelis, J. N., Saidani, M., Khorami, M., & Abbey, S. J. (2018). Investigation of intrinsic de-bonding in bonded concrete overlays: Material characterisation and numerical Study. *Engineering Solid Mechanics*, *6*(2), 155-174.

Piel, W., & Hanswille, G. (2006). Composite shear head systems for improved punching shear resistance of flat slabs. In *Composite Construction in Steel and Concrete V* (pp. 226-235).

Selby, R.G., & Vecchio, F.J. (1993). 3D constitutive relations for reinforced concrete, Tech, Rep.93-02, Department of Civil Engineering, Toronto, Canada.

Vecchio, F. J., & Collins, M. P. (1986). The modified compression-field theory for reinforced concrete elements subjected to shear. *ACI J.*, *83*(2), 219-231.

Xu, F., Chen, J., & Jin, W. L. (2016). Punching shear failure of concrete-filled steel tubular CHS connections. *Journal of Constructional Steel Research*, *124*, 113-121.

Yan, P. Y., & Wang, Y. C. (2016). Hybrid steel tubular column/flat slab construction—Development of a shearhead system to improve punching shear resistance. *Journal of Constructional Steel Research*, *119*, 154-168.